Vol. 26(3):489-499 | Ocean and Polar Research | September 2004

Article

Characteristics of the Polar Ionosphere Based on the Chatanika and Sondrestrom Incoherent Scatter Radars

Young-Sil Kwak[1]* and Byung-Ho Ahn[2]

[1]*Department of Astronomy and Atmospheric Science, Kyungpook National University*
[2]*Department of Earth Science, Kyungpook National University*
Daegu 702-701, Korea

Abstract : The climatological characteristics of the polar ionospheric currents obtained from the simultaneous observations of the ionospheric electric field and conductivity are examined. For this purpose, 43 and 109 days of measurements from the Chatanika and Sondrestrom incoherent scatter radars are utilized respectively. The ionospheric current density is compared with the corresponding ground magnetic disturbance. Several interesting characteristics about the polar ionosphere are apparent from this study: (1) The sun determines largely the conductance over the Sondrestrom radar, while the nighttime conductance distribution over the Chatanika radar is significantly affected by auroral precipitation. (2) The regions of the maximum N-S electric field over the Chatanika radar are located approximately at the dawn and dusk sectors, while they tend to shift towards dayside over the Sondrestrom radar. The N-S component over Sondrestrom is slightly stronger than Chatanika. However, the E-W component over Chatanika is negligible compared to that of Sondrestrom. (3) The E-W ionospheric current flows dominantly in the night hemisphere over Chatanika, while it flows in the sunlit hemisphere over Sondrestrom. The N-S current over Chatanika flows prominently in the dawn and dusk sectors, while a strong southward current flows in the prenoon sector over Sondrestrom. (4) The assumption of infinite sheet current approximation is far from realistic, underestimating the current density by a factor of 2 or more. It is particularly serious for the higher latitude region. (5) The correlation between ΔH and J_E is higher than the one between ΔD and J_N, indicating that field-aligned current affects ΔD significantly.

Key words : ionospheric conductance, electric field, current density, ground magnetic disturbance

1. Introduction

Since they came into operation in the 1960s, incoherent scatter radars have contributed significantly in advancing our understanding of the polar ionosphere, as well as the solar wind-magnetosphere-ionosphere coupling. In particular, it is possible to deduce the ionospheric current from estimates of the electric field and height profiles of the conductivity by incoherent scatter radar observations. Brekke *et al.* (1974) compared the ionospheric current estimated from the electric field and conductivity from the Chatanika radar with the ground magnetic variation at College. They found that the H component of the ground magnetic variation is in good agreement with the estimated east-west current, while the D component disagrees with the north-south current, thus indicating that the effect of the field-aligned current should be taken into account. Kamide and Brekke (1975) made a similar analysis using the Chatanika radar and showed that the infinite sheet current model almost always underestimates the current density by a factor of 2 of more. They noted that the latitudinal width of the auroral electrojet, the distance from the center of the electrojet, the latitudinal dependence (i.e., gradient) of the current density, and the field-aligned current also contribute to the underestimation. From data collected by the European Incoherent Scatter (EISCAT) radar and ground magnetic variation data, Araki *et al.* (1989) showed that ground magnetic variations are caused mainly by the Hall current and the contribution of the Pedersen current is no larger than 30% that of the Hall current.

*Corresponding author. E-mail : ys-kwak@hanmail.net

Chapman and Bartels (1940), Brekke *et al.* (1974) and Kamide and Brekke (1975) reported that magnetic variations observed on the Earth's surface are caused by the effect of an inducted current within the Earth's interior. Popov *et al.* (2001) attempted to separate contributions to the observed geomagnetic variations from external (ionospheric) and internal (induced) sources. Tanskanen *et al.* (2001) showed that the internal contribution peaks at substorm onset amounted to 40% of the total field, and reaches 10~20% after the maximum phase to the quiet level.

Ahn *et al.* (1999) showed the climatological characteristics of the auroral ionosphere, in terms of the electric field and ionospheric conductivity, were based on the Chatanika radar measurements. They reported that the Hall conductance distribution associated with the eastward electrojet in the post-noon sector is mainly determined by the Sun, while the one associated with the major part of the westward electrojet in the midnight-post-midnight sector was controlled by precipitating electrons. Thus, they pointed out that the eastward and westward electrojets are governed by different physical processes.

However, the study using the Chatanika and EISCAT radars is confined to only the auroral ionosphere. Fortunately, since Sondrestrom radar, which has been operated in Sondre Stromfjord, Greenland, from 1983, is located at a similar geographic latitude to the Chatanika and EISCAT radars, but at a higher geomagnetic latitude than that of the two radar. It is located in the polar cap region as well as the auroral region depending on the geomagnetic activity level. Thus, the Sondrestrom radar measurements including the Chatanika provide us with an opportunity to study the polar cap and the auroral region at the same time. Moreover, since the radars were operated over an extended period, the accumulated data is sufficient to extract some important climatological aspects of the polar ionosphere.

In this study, we examine diurnal variations in the ionospheric currents obtained by combining the ionospheric conductance and electric field from measurements taken by the Chatanika and Sondrestrom radars, which cover approximately the entire auroral and polar cap regions. The ionospheric current density is compared with the corresponding ground magnetic disturbance.

2. Database

The ionospheric conductivity and the electric field measurements utilized in this study were obtained from the Chatanika radar (geographic latitude, longitude: 65.10°N, 147.45°W; geomagnetic latitude, longitude: 64.75°N, 105.00°W) for a total of 43 days between 1977 and 1983 and the Sondrestrom radar (geographic latitude, longitude: 66.90°N, 50.90°W; geomagnetic latitude, longitude: 74.36°N, 42.40°W) for 109 days between 1983 and 1999. The Chatanika radar takes about 16 min to make a three-position measurement in the azimuthal direction, while maintaining an elevation angle somewhere between 60° and 80°. The electron density distribution within the altitude range of 90 and 200 km is used to estimate the height-integrated conductivity, i.e., conductance. Thus, the diameter of the field view of the radar, corresponding to the spatial resolution of the data, is about 140 km. The temporal resolution is about 16 min, the scan period of the radar. The 43 days of the Chatanika radar measurements in this study were 14 days in spring (February, March, and April), 7 days in summer (May, June, and July), 12 days in autumn (August, September, and October), and 10 days in winter (November, December, and January). The mean *Kp* index for the 43 days was 2+~3–. The typical observational mode of the Sondrestrom radar between 1983 and 1989 was that of a magnetic meridional scan mode along the –27° azimuth. The temporal resolution is about 5 min. The Sondrestrom radar between 1990 and 1999 maintained an elevation angle somewhere between 70° and 80°, while making a three-position measurement in the azimuthal direction. The temporal resolution is about 15 min, namely the scanning period of the radar. The electron density measurements for deducing the conductance were made within the altitude range of 90 and 200 km. A total of 109 days of Sondrestrom radar measurements in this study were 14 days in spring, 35 days in summer, 32 days in autumn, and 28 days in winter. The mean *Kp* index for the 109 days was 2+~3–.

The magnetic field was estimated based on the IGRF-1995 model (Barton 1997). The MSIS-90 model (Hedin 1991) was used in taking the neutral densities and temperatures used to drive ion-neutral and electron-neutral collision frequencies in estimating the conductivity. Besides the data mentioned above, the daily 10.7-cm solar radio flux, i.e., Sa values, and *Ap* index are also used to estimate the conductivity associated with solar EUV radiation.

The ground magnetic disturbance data to be compared with the ionospheric currents over Chatanika were from College, which is located roughly 33 km magnetic south of the Chatanika radar. The ionospheric currents over Sondrestrom were compared with those of the Sondrestrom magnetometer, which is being operated at the same site as the Sondrestrom radar. Before being compared with the

currents, the magnetic disturbance data was processed to average it with the temporal resolution of the radar data.

3. Climatological characteristics of the polar ionosphere

Ionospheric conductance distribution

The magnetic local time (MLT) variation of the conductance obtained from the radar measurements is examined, where the conductance is calculated by integrating the conductivities over the height range of 90 to 200 km.

Fig. 1(a) is the Hall conductance distribution over the Sondrestrom radar by superposing the entire 109-day measurements. One can easily see that the sun determines the conductance over Sondrestrom for the most part, which varies and maximizes near the local noon sector, although there is sporadic conductance enhancement associated with auroral particle precipitation before 0600 MLT and after 1500 MLT.

Fig. 1(b) shows the Hall conductance constructed by superposing the entire 43-day measurements from the Chatanika radar. As Ahn *et al.* (1999) already pointed out that one can notice that the Hall conductance distribution associated with auroral particle precipitation is not only significantly high at night, reaching a maximum around midnight local time, but also shows an extended region of high conductance over the morning hemisphere. On the other hand, the Hall conductance distribution is mainly due to solar EUV radiation in the post-noon sector from noon to around 1800 MLT.

The Pedersen conductance distributions over the Sondrestrom and Chatanika radars are also examined and shown in Figs. 1(c) and 1(d), respectively. The patterns of the Pedersen conductance distributions are similar to those of the Hall conductance distributions, except that the magnitudes of the Pedersen conductance are larger than those of the Hall conductance.

Electric field distribution

The magnetic local time variations of the electric fields over the Sondrestrom and Chatanika radars are examined in the same way as the conductance and shown in Fig. 2. One can see that the scatter from Sondrestrom extremes are unlike Chatanika because the temporal resolution of the Chatanika radar measurements is about 16 min, while that of the Sondrestrom radar measurements is about 5 min, particularly between 1983 and 1989.

Fig. 2(a) shows the north-south electric field over Sondrestrom. In spite of occasional large values around midnight, one can see that the regions of the maximum southward and northward components over Sondrestrom tend to shift towards daytime, around 0800-0900 MLT and 1300-1400 MLT, respectively. And the minimum values are found in the pre-noon sector, around 1100 MLT. In

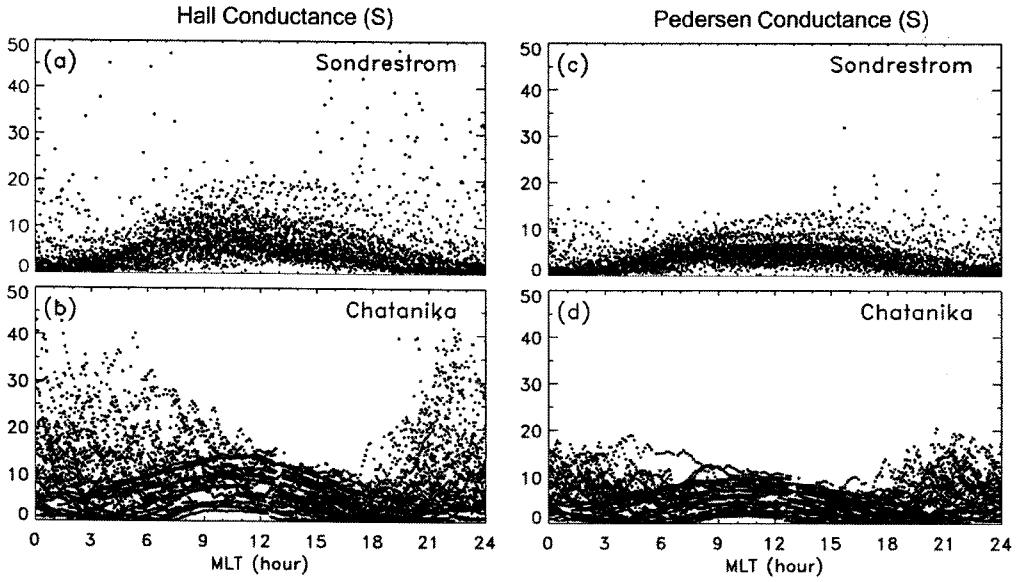

Fig. 1. (a) Diurnal distribution patterns of the Hall conductance estimated from the Sondrestrom radar observations for the entire 109 days. (b) Diurnal distribution patterns of the Hall conductance estimated from the Chatanika radar observations for the entire 43 days. (c) Same as Fig. 1(a), but for the Pedersen conductance distribution. (d) Same as Fig. 1(b), but for the Pedersen conductance distribution.

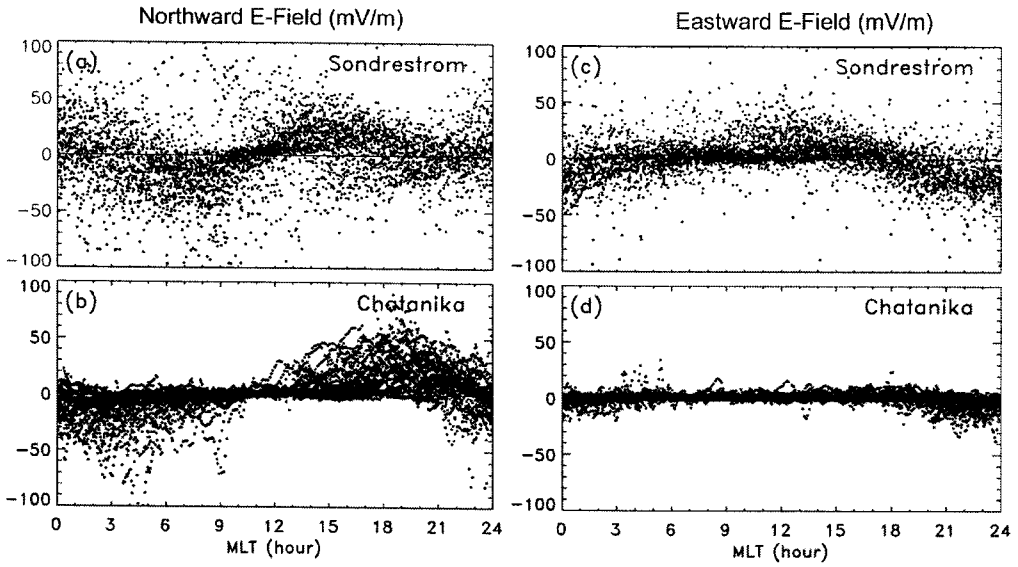

Fig. 2. (a) Diurnal distribution patterns of the north-south component of the electric field estimated from the Sondrestrom radar observations for the entire 109 days. (b) Diurnal distribution patterns of the north-south component of the electric field estimated from the Chatanika radar observations for the entire 43 days. (c) Same as Fig. 2(a), but for the east-west component of the electric field. (d) Same as Fig. 2(b), but for the east-west component of the electric field.

Fig. 2(b), the regions of the maximum southward and northward electric fields over the Chatanika radar are located approximately at dawn and dusk, around 0400-0500 MLT and around 1900-2000 MLT, respectively, as reported by Ahn *et al.* (1999). The characteristics of the north-south electric field around midnight of both Sondrestrom and Chatanika is that the frequencies of the two components are equal, suggesting the probabilities affecting the positive electric potential cell and the negative electric potential cell are generally equal around midnight.

Figs. 2(c) and 2(d) show the east-west electric field over Sondrestrom and Chatanika, respectively. The maximum eastward and westward components over Sondrestrom are found near the local noon sector and around midnight, respectively, and the strengths of the two components are nearly equal. On the other hand, the east-west electric field over Chatanika is generally weak, except for the pre-midnight sector, around 2200-2300 MLT with ~40 mV/m, and that is slightly weak by a factor of about 1/4 that of Sondrestrom.

4. Ionospheric current density distribution

According to the Ohm's law, the height-integrated eastward and northward current densities, J_E and J_N, can be written as follows

$$J_E = \Sigma_P E_E + \Sigma_H E_N \quad (1a)$$

$$J_N = \Sigma_P E_N - \Sigma_H E_E \quad (1b)$$

where E_E and E_N represent the eastward and northward components of the electric field, respectively, and Σ_H and Σ_P represent the height-integrated Hall and Pedersen conductivities. Since ionospheric conductance is obtained by integrating from 90 to 200 km, the resulting current densities are also integrated over the altitude range.

We estimated the ionospheric horizontal current densities by substituting the equations (1a) and (1b) with the conductance and electric field of Figs. 1 and 2, and showed J_E and J_N in Figs. 3 and 4, respectively.

Fig. 3(a) is the magnetic local time (MLT) variation of the east-west component of the current density over Sondrestrom, which is constructed by superposing the entire 109-day measurements. The eastward current flows generally in the afternoon sector including the pre-noon sector, 1000-1200-1900 MLT, and the westward current flows generally from the evening sector to the morning sector past midnight, 1900-0000-1000 MLT. To provide climatological characteristics, the average and the corresponding standard deviation of the east-west component for each MLT is shown in Fig. 3(b). The hourly mean maximum eastward and westward currents are found to be around 1300-1400 MLT with a magnitude of around +170 mA/m and around

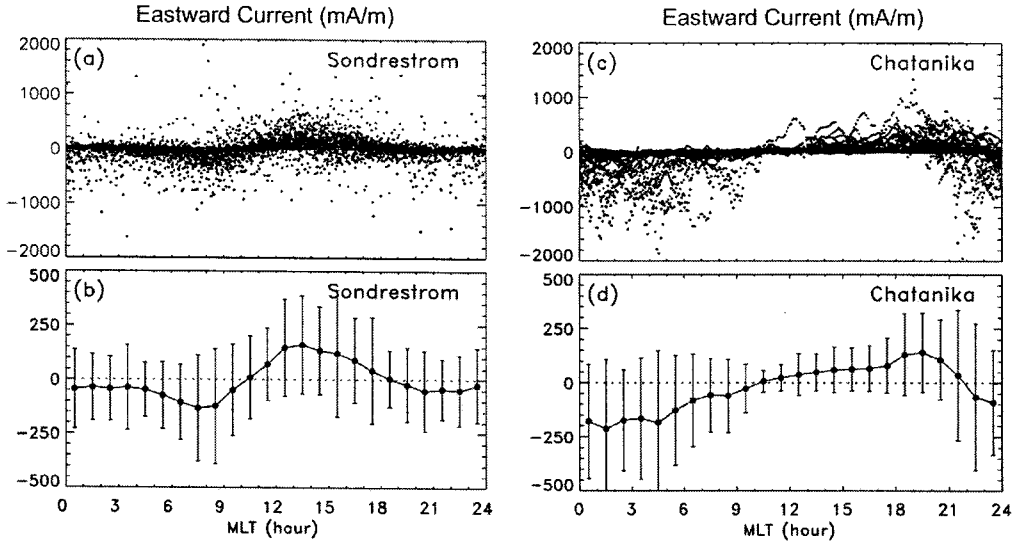

Fig. 3. (a) Diurnal distribution of the east-west component of the ionospheric current density over Sondrestrom estimated by combining the conductance and the electric field shown in Figs. 1 and 2, respectively. (b) Hourly mean value and corresponding standard deviation for each MLT using the entire data set of Fig. 3(a). (c) Diurnal distribution of the east-west component of the ionospheric current density over Chatanika. (d) Hourly mean value and corresponding standard deviation for each MLT using the entire data set of Fig. 3(c).

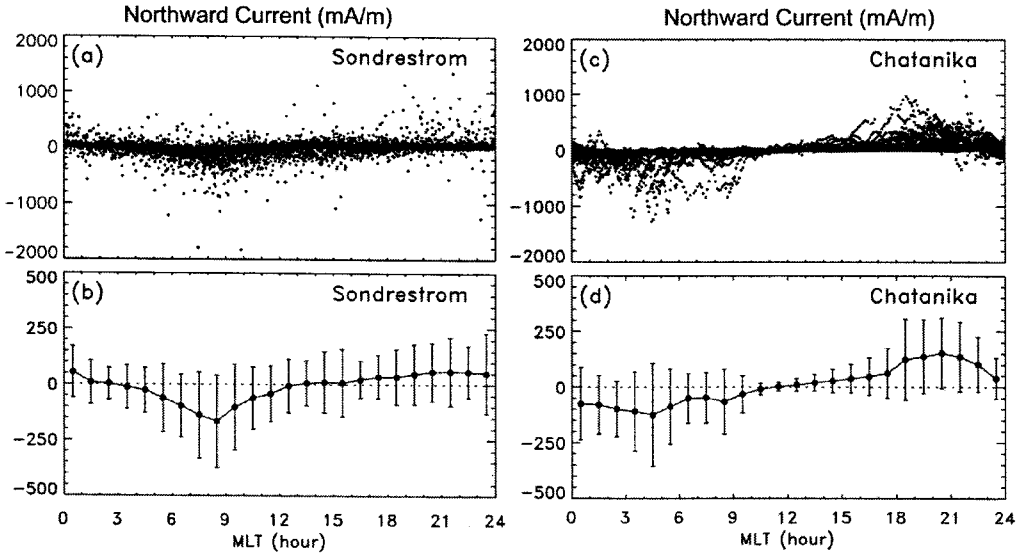

Fig. 4. Same as Fig. 3, but for the north-south component of the ionospheric current density.

0800-0900 MLT with a magnitude of around −140 mA/m, respectively. It is interesting to note that the east-west current over Sondrestrom shifts toward the hemisphere, 0600-1200-1800 MLT, rather than over Chatanika (see Figs. 3c and 3d).

Fig. 3(c) shows the east-west current over Chatanika constructed by superposing the entire 43-day measurements. The eastward current flows generally in the evening sector from about 1000 MLT to about midnight. The westward current flows generally in the morning sector and its western boundary expands as early as 2100 MLT. As expected, the westward current in the morning sector is generally higher than the eastward component in the evening sector. It is probably due to the fact that the variability in conductivity in the westward current is larger than that of the eastward current. As can be seen in Fig. 3(d), the hourly mean maximum eastward and westward currents are found to

be around 1900-2000 MLT with a magnitude of around +140 mA/m and around post-midnight with a magnitude of around −220 mA/m, respectively. The minimum values are found in the pre-noon sector, around 1000 MLT. Thus, one can see that the east-west ionospheric current over Chatanika flows dominantly in the night hemisphere, 1800 -0000-0600 MLT.

The north-south component of the current density over Sondrestrom is examined during the same time period shown in Fig. 3(a), and in Fig. 4(a). The entire pattern is characterized by a strong southward component in the pre-noon sector, around 0900-1000 MLT. It is clearly seen from Fig. 4(b), showing the hourly mean value, and the mean maximum southward current reaches around −170 mA/m.

The north-south current over Chatanika during the same time period shown in Fig. 3(c) is also examined in the same way as Sondrestrom. The results are shown in Fig. 4(c). The northward current flows generally in the evening sector about 1100-1200-2300 MLT. On the other hand, the southward current flows generally in the morning sector about 2300-0000-1100 MLT. From Fig. 4(d), which shows the hourly mean north-south current, one can see that the mean maximum northward and southward currents are found around dusk and dawn. The mean maximum magnitudes in the two sectors are around +150 mA/m and around −120 mA/m, respectively.

5. The relationship between ionospheric current and ground magnetic disturbance

The magnetic disturbances observed on the ground are the combined result of the ionospheric currents and the induced current within the earth. The magnetic disturbance (ΔB) associated with an infinite horizontal current sheet above a flat earth is

$$\Delta B = (1/f)(\mu_0/2)\ J \qquad (2)$$

where f denotes the induction effect within the earth. For non-conducting earth, f is 1, while for the perfectly conducting flat earth, f becomes 1/2. If we assume that f is 2/3 (Kamide and Brekke 1975), the relation between the infinite horizontal ionospheric current (J) and the observed geomagnetic disturbance ΔB can be approximated by ΔB = 0.95 J, where J and B are in mA/m and nT, respectively. Recently, Tanskanen *et al.* (2001) showed that the internal contribution peaks at substorm onset, amounting to ~ 40% of the total field, and reached 10~20% after the maximum phase to the quiet level. According to them, the relation between J and ΔB during the quiet time is ΔB = 0.70 − 0.79 J.

The magnetic local time distributions of the ground magnetic disturbance observed by the magnetometers are shown in Fig. 5. Fig. 5(a) is the H component measured by the Sondrestrom magnetometer during the same time period shown in Fig. 3(a). The northward variation is

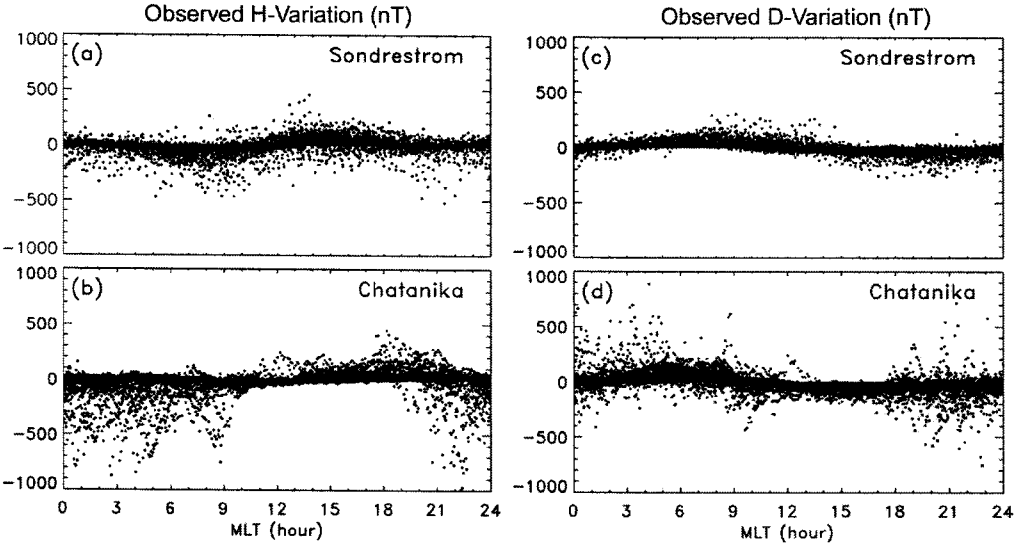

Fig. 5. (a) Diurnal distribution of the H component of the ground magnetic disturbance measured from the Sondrestrom magnetometer during the same time period shown in Fig. 3(a). (b) Diurnal distribution of the H component of the ground magnetic disturbance measured from the Chatanika magnetometer during the same time period shown in Fig. 3(c). (c) Same as Fig. 5(a), but for the D component distribution. (d) Same as Fig. 5(b), but for the D component distribution.

observed generally in the afternoon sector including the pre-noon sector, 1000-1200-1900 MLT. The southward variation is observed generally in the morning sector from midnight to about 1000 MLT. One can see that the H variation at Sondrestrom is observed in the sunlit hemisphere. Fig. 5(b) is the H component measured by the College

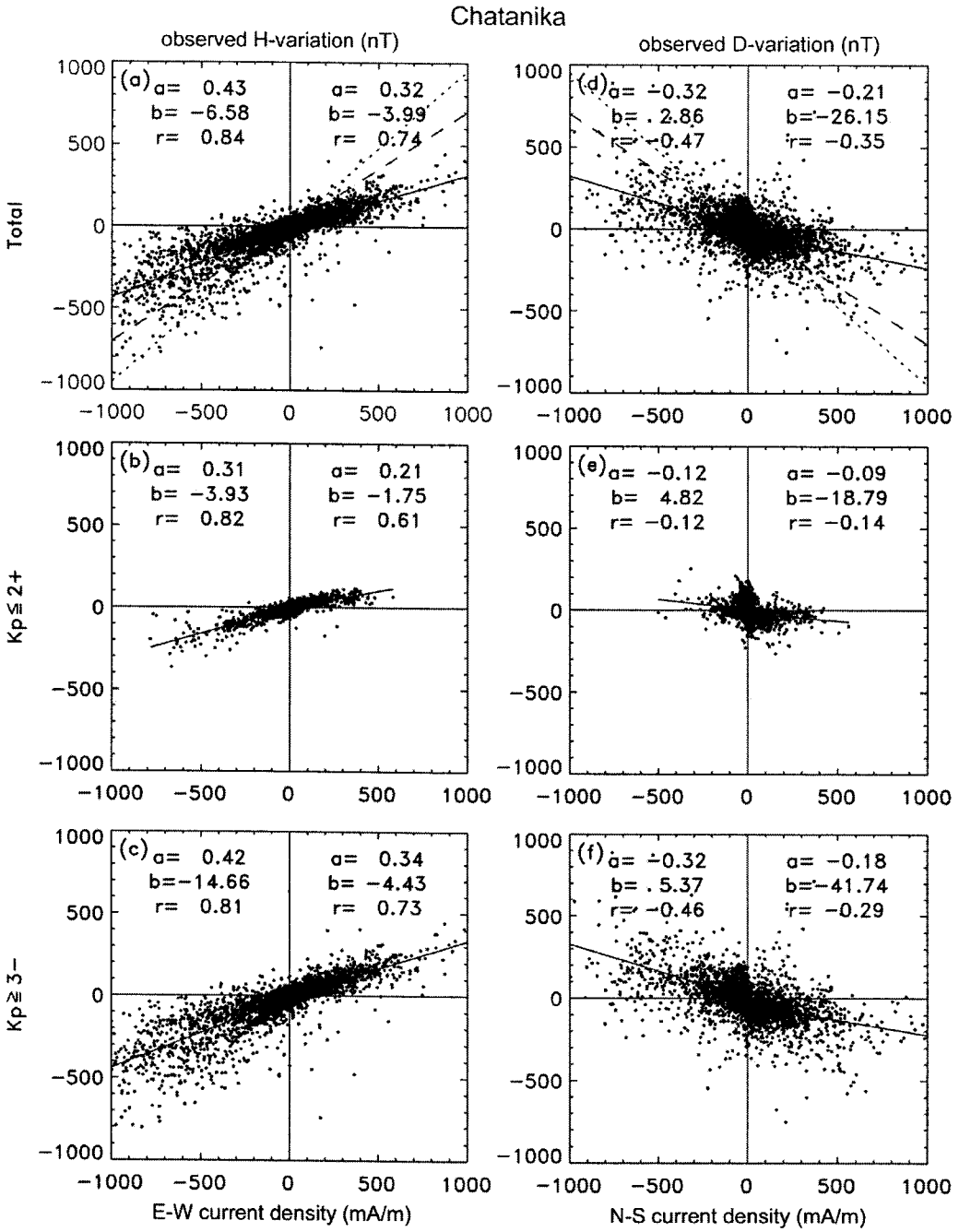

Fig. 6. Relationship between the height-integrated ionospheric current (J_E, J_N) estimated from the Chatanika radar and the corresponding ground magnetic disturbance at College (ΔH_{obs}, ΔD_{obs}). Here we represent the relation between the two physical quantities as the correlation coefficient, r, and the coefficients, a, b, of a linear fit, $\Delta H_{obs} = a\ J_E + b$ and $\Delta D_{obs} = a\ J_N + b$, where is given as the solid line. The linear relations based on the infinite overhead current approximation for $f = 2/3$ (Kamide and Brekke 1975) and 9/10 (Tanskanen *et al.* 2001) are also given as the dotted and dashed lines, respectively.

magnetometer during the same time period shown in Fig. 3(b). The northward variation is observed generally in the evening sector from 1000 MLT to around midnight. The southward variation is observed from the evening sector to the morning sector through midnight, 1900-0000-1000 MLT. One can see that the H variation at College is observed dominantly in the night hemisphere. The D component of the ground magnetic disturbance measured from the Sondrestrom magnetometer is shown in Fig. 5(c). The eastward variation is observed generally in the pre-noon sector including noon, and the westward variation is observed generally in the evening sector. The D component from College (Fig. 5d) is characterized by dominant eastward and westward variations in the dawn and dusk sectors, respectively.

The relationship between the height-integrated ionospheric currents (J_E, J_N) estimated from the Chatanika radar and the simultaneously obtained ground magnetic disturbance at College (ΔH_{obs}, ΔD_{obs}) is examined, and the results are shown in Fig. 6. Fig. 6(a) shows the relationship between J_E and ΔH_{obs}. The relation between the two physical quantities is placed in a linear relationship: $\Delta H_{obs} = a\ J_E + b$, where it is given as a solid line. The correlation coefficient r is also estimated. The correlation coefficients between J_E and ΔH_{obs} in the westward and eastward current regions are 0.84 and 0.74, respectively. This suggests that the ground magnetic H disturbances in the auroral zone are caused mainly by the east-west ionospheric current. However, it is interesting to note that the correlation coefficients are different in the westward and eastward current regions. Moreover, it is also interesting to note that the slopes a's are different in the westward and eastward electrojet regions with a's being 0.43 and 0.32, respectively. This means that the contributions of the westward and eastward currents to ΔH for the same region are different as 0.43 and 0.32 nT/(mA/m), respectively. The b values, ΔH value for J_E being 0, are also different in the westward and eastward electrojet regions with −6.58 and −3.99, respectively. In terms of comparisons, the linear relations based on the infinite overhead current approximation for $f = 2/3$ (Kamide and Brekke 1975) and 9/10 (Tanskanen *et al.* 2001) are also given as the dotted and dashed lines, respectively. From Fig. 6, one can also see that the assumption of infinite sheet current approximation is far from realistic, underestimating the east-west current density by a factor of 2 or more. It is clear that even the extreme approximation ($f = 9/10$) underestimates the current density by a large factor. It is more serious for the eastward current region than in the westward current region. The underestimate of infinite sheet current approximation and the deference of the linear relation between J_E and ΔH_{obs} in the westward and eastward electrojet regions resulted from the fact that the real ionospheric sheet current is not an infinite current but one flowing within a finite range along the auroral oval, and is constructed by the latitudinal width of the auroral electrojet, the distance from the center of the electrojet and the latitudinal dependence (i.e., gradient) of the current density.

Figs. 6(b) and 6(c) show how the relation between J_E and ΔH_{obs} changes with magnetic activity. During quiet periods for $Kp \leq 2+$ (Fig. 6b) the slopes, the a's, are 0.31 and 0.21 in the westward and eastward electrojet regions, respectively. That is, the contributions of westward and eastward currents to ΔH are 0.31 and 0.21 nT/(mA/m), respectively. On the other hand, during disturbed periods for $Kp \geq 3-$ (Fig. 6c) the slopes known as the a's are 0.42 and 0.34 in the westward and eastward electrojet regions, respectively. This represents the contributions of westward and eastward currents to ΔH are 0.42 and 0.34 nT/(mA/m), respectively. As the magnetic activity intensifies further, the contribution of the east-west ionospheric current to ΔH is larger, and the correlation coefficient becomes larger although the change of r in the westward current region is not shown. Thus, the underestimate of the infinite sheet current density is more serious during the quiet period with auroral electrojet retreating poleward.

The relationship between J_N and ΔD_{obs} for Chatanika is also examined. The results are shown in Fig. 6(d), where the relation between the two physical quantities fits into a linear relationship: $\Delta D_{obs} = a\ J_N + b$. The correlation coefficients between J_N and ΔD_{obs} in the southward and northward electrojet regions with −0.47 and −0.35, respectively, are worse than those between J_E and ΔH_{obs} (see Fig. 6a), indicating that the field-aligned current affects ΔD significantly. Moreover, the slopes of a's showing a linear relationship are −0.32 and −0.21 in the southward and northward electrojet regions, respectively, and are therefore lower than those between J_E and ΔH_{obs}. If one considers the fact that the southward current region is nearly the same for the morning sector as that for the westward currents region, and the northward current region is nearly the same for the evening sector as that for the eastward current region, this means that ΔD is seen to be considerably weaker than ΔH by the ionospheric current over the same region. In reality, since J_N associated with ΔD is connected to the field-aligned current, the ground ΔD is combined with the results of J_N and the field-aligned current. In the morning sector, the region 1 currents on the poleward side flow into the ionosphere and the region 2 currents on the equatorward side flow out of the ionosphere. The flow pattern is reversed

in the evening sector (Iijima and Potemra 1976). In the morning sector ΔD caused by the region 1 and 2 currents displays a westward variation, and therefore weakens the eastward ΔD caused by the southward J_N. On the other hand, in the evening sector ΔD caused by the region 1 and 2 currents an eastward variation is displayed, and it also weakens the westward ΔD caused by the northward J_N. From Fig. 6(d), we notice that there are points in the first and third quadrants unlike the case for the relation between J_E and ΔH. These points are also considered to be the result of the field-aligned current. As in the relation between J_E and ΔH, for sake of comparison, the linear relations

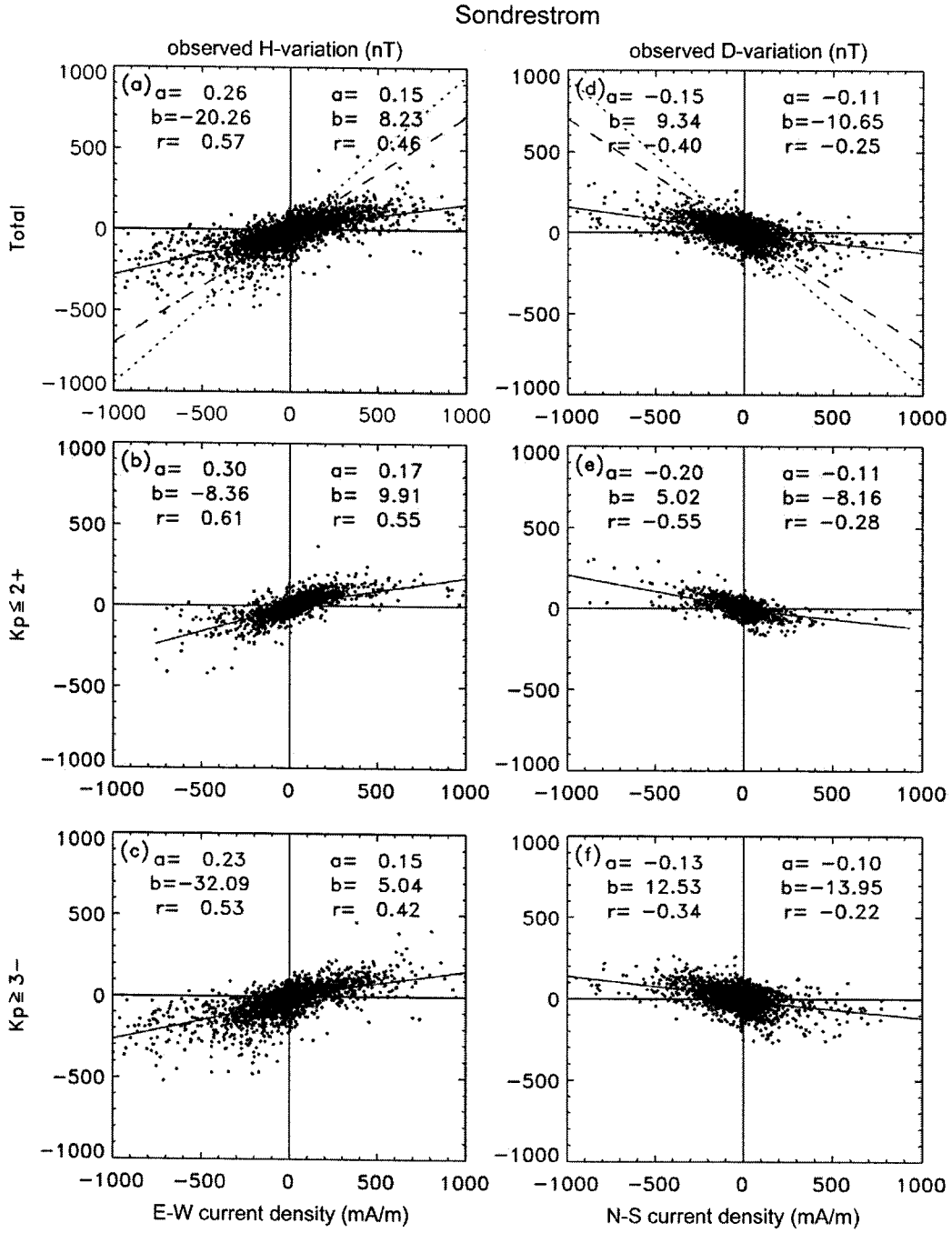

Fig. 7. Same as Fig. 6, but for relationship between the height-integrated ionospheric current (J_E, J_N) estimated from the Sondrestrom radar and the corresponding ground magnetic disturbance at Sondrestrom (ΔH_{obs}, ΔD_{obs}).

based on the infinite overhead current approximation for $f = 2/3$ (Kamide and Brekke 1975) and 9/10 (Tanskanen *et al.* 2001) are also given as the dotted and dashed lines, respectively. One can see that the assumption of infinite sheet current approximation for J_N-ΔD is far less realistic than that for J_E-ΔH, where the current density is more underestimated than that for J_E-ΔH. This is the reason for the gross underestimate for J_E-ΔH and the effect of the field-aligned current.

The change in the relation between J_N and ΔD_{obs} in terms of magnetic activity is shown in Figs. 6(e) and 6(f). The correlation coefficients in the southward and northward current regions are –0.12 and –0.14 during quiet periods, respectively, and –0.46 and –0.29 during disturbed periods, respectively. One can see that, as the magnetic activity intensifies further, the correlation between the two quantities becomes better. The sloping a's in the southward and northward current regions are –0.12 and 0.09 during the quiet period, respectively, and –0.32 and –0.18 during the disturbed period, respectively. With the enhancement of magnetic activity, the contribution of the north-south ionospheric current to ΔD increases by a factor of 2 or more. From Fig. 6(d), it is worthy of notice that during quiet periods there are large ΔD values for very small J_N, indicating that the neutral wind seems to play an important role particularly when it comes to north-south ionospheric currents.

Fig. 7 shows the relationship between the height-integrated ionospheric currents (J_E, J_N) estimated from the Sondrestrom radar and the simultaneously obtained ground magnetic disturbance (ΔH_{obs}, ΔD_{obs}) measured by Sondrestrom magnetometer. In Fig. 7(a), showing the relation between J_E and ΔH_{obs}, the correlation coefficients between the two physical quantities for Sondrestrom are 0.57 and 0.46 in the westward and eastward current regions, respectively, and smaller than those for Chatanika (see Fig. 6a). Moreover, the slopes displaying the linear relationship are 0.26 and 0.15 in the westward and eastward current regions, respectively, and smaller by a factor of about 2 than those for Chatanika. That is, the contribution of east-west ionospheric current over Sondrestrom to ΔH is smaller by a factor of about 2 than that at Chatanika. This suggests that underestimation of the infinite sheet current approximation is more serious for Sondrestrom than for Chatanika.

Figs. 7(b) and 7(c) show the change in the relationship between J_E and ΔH_{obs} in terms of magnetic activity. The correlation coefficients between the two quantities in the westward and eastward current regions are 0.61 and 0.55 during quiet periods, respectively, and 0.53 and 0.42 during disturbed periods, respectively. As the magnetic activity level increases, the correlation between J_E and ΔH for Sondrestrom deteriorates unlike the case for Chatanika becoming better with the enhancement of magnetic activity (see Figs. 6b and 6c). The sloping a's in the westward and eastward current regions, are 0.30 and 0.17 during the quiet period, respectively, and 0.23 and 0.15 during the disturbed period, respectively. With enhancement of magnetic activity, the contribution of the east-west ionospheric current to ΔH for Sondrestrom becomes lower unlike the case for Chatanika.

Fig. 7(d) shows the relationship between J_N and ΔD_{obs} for Sondrestrom. As expected due to the effect of the field-aligned current, one can see that the correlation between J_N and ΔD and the slope are lower than those between J_E and ΔH (see Fig. 7a). And they are also lower than those between J_N and ΔD for Chatanika (see Fig. 6d).

The change of the relationship between J_N and ΔD_{obs} with magnetic activity for Sondrestrom is shown in Figs. 7(e) and 7(f). One can see that the correlation coefficient and the slope decrease with the enhancement of magnetic activity unlike the case for Chatanika, which becomes higher according to the activity level.

6. Summary and discussion

The climatological characteristics of the polar ionosphere are examined in terms of the ionospheric conductance and the electric field. For this purpose, 43 and 109 days of measurements from the Chatanika and Sondrestrom incoherent scatter radars are utilized, respectively. By combining these two quantities, it is possible to deduce the overhead ionospheric current distributions. The ionospheric current density thus obtained is compared with the corresponding ground magnetic disturbance. Also estimated is the effect of the field-aligned current on the ground magnetic disturbance, particularly on the D component. Several interesting climatological characteristics about the polar ionosphere are apparent from this study. (1) Ionospheric conductance in the dayside is dominated by solar EUV radiation. The sun determines largely the conductance over the Sondrestrom radar, while the nighttime conductance distribution over the Chatanika radar is significantly affected by auroral precipitation. (2) The regions of the maximum N-S electric field over the Chatanika radar are located approximately at the dawn and dusk sectors, while they tend to shift towards the dayside over the Sondrestrom radar. The E-W component over Sondrestrom is slightly stronger than Chatanika. However, the E-W component over Chatanika is negligible compared to that of Sondrestrom. (3) The

E-W ionospheric current over Chatanika flows dominantly in the night hemisphere, 1800-0000-0600 MLT, while flowing in the sunlit hemisphere, 0600-1200-1800 MLT over Sondrestrom. The N-S current over Chatanika flows prominently in the dawn and dusk sectors, while a strong southward current flows over Sondrestrom in the pre-noon sector. (4) The assumption of infinite sheet current approximation is far from realistic, underestimating the current density by a factor of 2 or more. It is particularly serious for higher latitude regions and during quiet periods with auroral electrojet retreating poleward. And the induction effect from the earth is probably very small, 10~20% (Tanskanen *et al.* 2001). Thus, one should be cautious in inferring ionospheric current distribution from ground magnetic disturbance data. (5) The correlation between ΔH and J_E is higher than that observed between ΔD and J_N, indicating that field-aligned current significantly affects the ΔD. During quiet periods, neutral winds seem to play a decisive role, particularly in the case of the N-S ionospheric current.

Acknowledgements

We thank B.A. Emery for helping to use CEDAR Database. We also thank J.P. Thayer and M. McCready at SRI for supplying the Sondrestrom incoherent scatter radar data, and J. Watermann at DMI for supplying the magnetic observatory data.

References

Ahn, B.-H., B.A. Emery, H.W. Kroehl, and Y. Kamide. 1999. Climatological characteristics of the auroral ionosphere in terms of electric field and ionospheric conductance. *J. Geophys. Res.*, 104, 10031-10040.

Araki, T., K. Schlegel, and H. Luhr. 1989. Geomagnetic effects of the Hall and Pedersen current flowing in the auroral ionosphere. *J. Geophys. Res.*, 94, 17185-17199.

Barton, C.E. 1997. International geomagnetic reference field: The seventh generation. *J. Geomag. Geoelectr.*, 49, 123-148.

Brekke, A., J.R. Doupnik, and P.M. Banks. 1974. Incoherent scatter measurement of E region conductivities and current in the auroral zone. *J. Geophys. Res.*, 79, 3773-3790.

Chapman, S. and J. Bartels. 1940. Geomagnetism, Vol. 1. Clarendon, Oxford.

Hedin, A.E. 1991. Extension of the MSIS thermospheric model into the middle and lower atmosphere. *J. Geophys. Res.*, 82, 2851-2853.

Iijima, T. and T.A. Potemra. 1976. The amplitude distribution of field-aligned currents at northern high latitude observed by TRIAD. *J. Geophys. Res.*, 81, 2165-2174.

Kamide, Y. and A. Brekke. 1975. Auroral electrojet current density deduced from the Chatanika radar and from the Alaska meridian chain of magnetic observatories. *J. Geophys. Res.*, 80, 587-594.

Kamide, Y., S.-I. Akasofu, and A. Brekke. 1976. Ionosphere current obtained from the Chatanika radar and ground magnetic perturbations at the auroral latitude. *Planet. Space Sci.*, 24, 173-201.

Kamide, Y., W. Sun, and S.-I. Akasofu. 1996. The average ionospheric electrodynamics for the different substorm phases. *J. Geophys. Res.*, 101, 99-109.

Popov, V.A., V.O. Papitashvili, and J.F. Watermann. 2001. Modeling of equivalent ionospheric currents from meridian magnetometer chain data. *Earth Planets Space*, 53, 129-137.

Tanskanen, E.I., A. Viljanen, T.I. Pulkkinen, R. Pirjola, L. Häkkinen, A. Pulkkinen, and O. Amm. 2001. At substorm onset, 40% of AL comes from underground. *J. Geophys. Res.*, 106, 13119-13134.

Received Jun. 10, 2004
Accepted Aug. 2, 2004